Available online at www.sciencedirect.com
SCIENCE DIRECT®
Catena 55 (2004) 49–77
CATENA
www.elsevier.com/locate/catena

Scale dependency in spatial patterns of saturated hydraulic conductivity

J.A. Sobieraj[a,*], H. Elsenbeer[b], G. Cameron[c]

[a] *Department of Civil and Environmental Engineering, University of Cincinnati, Cincinnati, OH 45221-0071, USA*
[b] *Institute of Geoecology, University of Potsdam, P.O. Box 60 15 53, 14415 Potsdam, Germany*
[c] *Department of Biological Sciences, University of Cincinnati, Cincinnati, OH 45221-0006, USA*

Received 12 December 2002; accepted 25 April 2003

Abstract

This study investigates spatial patterns of Ks and tests the hypothesis of whether structural variance emerges from noise with increasing sampling precision. We analyzed point measurements of Ks along independent transects at sampling intervals of 25, 10, 1 and 0.25 m. The field area is a tropical rainforest catena (i.e. toposequence) characterized by systematic downslope changes in soil properties including color (red to yellow), mineralogy (kaolinite–illite to kaolinite) and texture (sandy clay to sand). Independent transects spanning the entire catena at lag intervals of 25 and 10 m reveal little to no spatial patterns in Ks; i.e. scatter plots are noisy and lack apparent spatial trends, and semivariograms suggest little to no autocorrelation in Ks. As sampling precision is increased ($h = 1$ and 0.25 m), spatial patterns emerge in Ks for the downslope areas, in which distinctive hydraulic boundaries in Ks correlate with relatively small-scale, topography-controlled soils with coarse textures ($\geq 80\%$ sand). For these areas, semivariograms of Ks and those of %sand and %clay exhibit similar spatial structure characterized by small nugget variances and large ranges, and nugget variance is reduced as sampling precision increases from 1 to 0.25 m. In the upslope, clay-rich locations along this toposequence, Ks exhibits few spatial patterns, irrespective of sampling scale. For these locations, scatter plots are noisy without apparent spatial trends, and semivariograms show almost complete nugget variance, suggesting little to no correlation in this hydraulic parameter at any scale. This study suggests that in the absence of coarse textures ($\geq 80\%$ sand), there is little predictability in Ks, even at sampling intervals of 0.25 m. We believe this lack of spatial

* Corresponding author. Preventive Medicine Service, Industrial Hygiene Section, William Beaumont Army Medical Center, Building 7304, 5005 N. Piedras Street, El Paso, TX 79920-5001, USA. Fax: +1-915-569-3181.
E-mail address: Josef.Sobieraj@amedd.army.mil (J.A. Sobieraj).

doi:10.1016/S0341-8162(03)00090-0

structure is due to a predominance of small-scale processes such as biological activity that largely control Ks in this forested setting.

Keywords: Amazon Basin; Catena; Saturated hydraulic conductivity; Scale; Spatial variability; Tropical rainforest

1. Introduction

Saturated hydraulic conductivity (Ks) is a challenging soil hydraulic property to describe because it can change many orders of magnitude over short distances. Heterogeneity of soil properties within and between soil horizons causes some regions to be more or less favorable to flow, and even the style of flow is highly variable with extremes represented by tortuous flow between individual particles and rapid flow through large, continuous macropores. Variability of Ks in soils has been viewed with respect to the numerous independent processes operating at different spatial and temporal scales that McBratney (1998) describes in terms of a nested hierarchy. High levels in this hierarchy are characterized by large spatial and temporal scales, whereas low levels are characterized by small spatial and temporal scales. Examples of high to intermediate levels include topography and mappable soil units, and at these levels, Ks is commonly assigned a single value over large areas in catchment models (e.g. Davis et al., 1999). Examples of low levels include biological processes, which can have a profound influence in controlling water movement. For example, studies have shown that infiltration rates over ant nests are approximately four to nine times higher than those of control soils and can exceed 1000 mm h^{-1} (Eldridge, 1994; Lobry de Bruyn and Conacher, 1994), and Lee (1985) lists studies about the influence of earthworm activities on soil properties.

Recognizing that Ks represents an end result of a number of independent processes whose complex interactions we are presently incapable of fully describing, deterministic methods for describing the spatial continuity of Ks are impractical. Therefore, a popular alternative is the use of stochastic (probabilistic) models in which the data are assumed to be the result of a random process, and model estimation is based on the mean and variance of a linear combination of random variables (see Isaaks and Srivastava, 1989 for review). A basic assumption in stochastic analysis is that the variance of increments, commonly represented in the form of a variogram, is bounded by the property's variance (Journel and Huijbregts, 1978), and examples of Ks studies using semivariograms include Lauren et al. (1988), Wilson et al. (1989), Mohanty et al. (1994), Mallants et al. (1996, 1997), Buttle and House (1997), Bosch and West (1998), and Mohanty and Mousli (2000).

Burrough (1983a,b) evaluated scale dependency in the variability of a number of soil properties (but not Ks) and noted that it was the scale of observation that determined if spatial variations were regarded as either interpretable signal (structure) or uninterpretable noise. The distinction between structure and noise is entirely scale-dependent because increasing the scale of observation almost always reveals structure in the noise. A toposequence (i.e. catena) represents an orderly pattern of soil properties in space with

topography as the primary controlling factor. Sobieraj et al. (2002) investigated if Ks exhibited a similar functional distribution in space as other soil properties (i.e. color, mineralogy, texture, etc.) along a tropical rainforest catena. At the hillslope scale at large sampling intervals ($h = 25$ m), statistical analyses suggest that Ks is uncorrelated at this scale (uninterpretable noise). This paper investigates the relationship between spatial structure and noise for Ks at different sampling scales. Specifically, the objectives of this

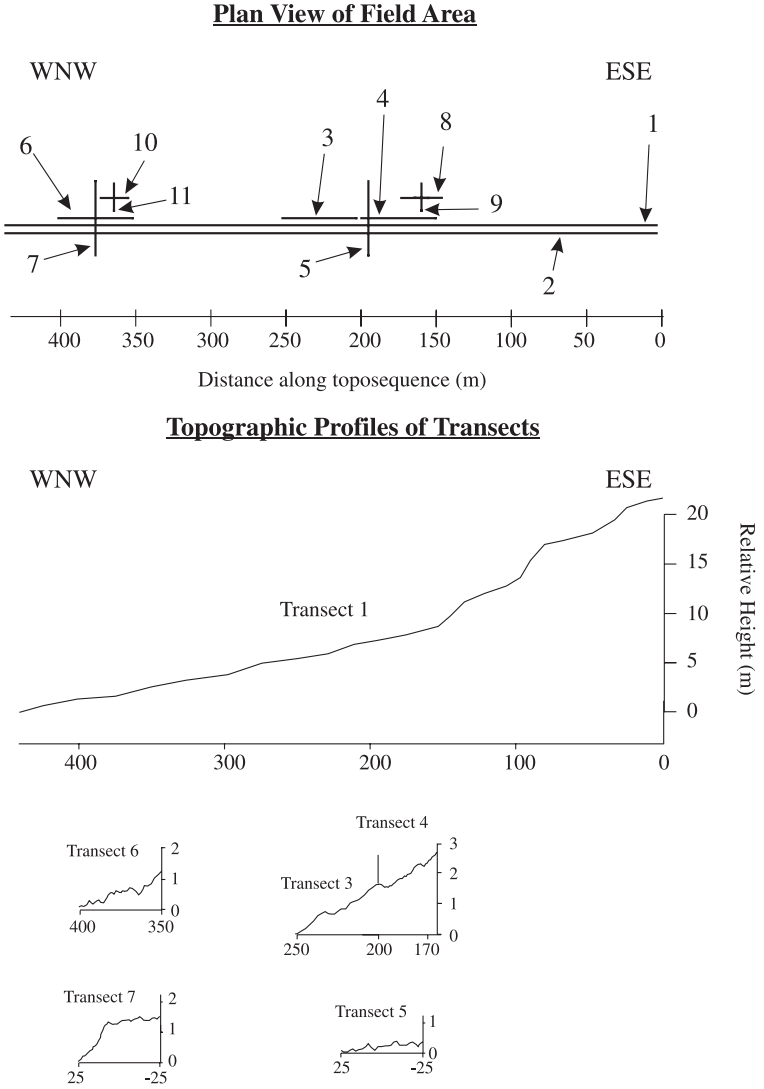

Fig. 1. Plan view showing configuration of 11 transects, and cross-sectional view showing topographic profiles of transects for this study.

paper are to: (1) determine if spatial structure in Ks emerges from noise with increased sampling precision, (2) evaluate if spatial patterns in Ks, the hydraulic property, can be linked with spatial patterns of soil physical properties, and (3) evaluate linkages between small-scale biological processes and spatial structure of Ks.

2. Research site

The research site is located in undisturbed tropical rainforest at Rancho Grande (10°18′S, 62°52′W, 143 m a.m.s.l.) in the state of Rondônia, Brazil. Mean air temperature is approximately 27 °C, and mean annual precipitation 2265 mm (H. Schmitz, personal communication). The prevailing lithology is Precambrian gneiss, which has weathered to a low-relief landscape with long, smooth, convex slopes and intervening, steep, NNE–SSW trending ridges as high as 500 m a.m.s.l. Fig. 1 shows a 440-m-long research transect consisting of a catenary sequence described by Sobieraj et al. (2002), in which the salient features are a downslope textural shift from fine to coarse, a color shift from red to yellow, and a shift from a kaolinitic–illitic to a pure kaolinitic clay mineralogy.

3. Methods

Fig. 1 shows the experimental design consisting of 11 transects, and Table 1 provides information on transect length, lag interval (h) and sampling depths used for measuring Ks. The 11 independent transects occur at different lag intervals, which allows for the evaluation of spatial patterns of Ks at different sampling scales. For example, transects 1

Table 1
Transect and sampling information

Transect information			Borehole depth (cm)			
ID	Lag (m)	Length	12.5	20	50	100
1	25	440	×	×	×	NA
2	10	440	× [a]	×	× [a]	NA
3[b]	0.25, 1	50	×	×	×	×
4	1	50	× [a]	×	× [a]	× [a]
5	1	50	×	×	×	×
6	1	50	× [a]	×	× [a]	× [a]
7	1	50	×	×	×	×
8	0.25	20	×	×	×	×
9	0.25	20	×	×	×	×
10	0.25	20	×	×	×	×
11	0.25	20	×	×	×	×

NA indicates that shallow bedrock precluded measurement of Ks.

[a] This indicates soil samples collected from borehole used for measuring Ks at following depth intervals: 0–12.5, 40–50, and 90–100 cm.

[b] Transect 3 sampled at 0.25-m lags at depths of 12.5 and 100 cm, and lags of 1 m at 20 and 50 cm depths.

and 2, which span the entire 440-m toposequence at lags of 25 and 10 m, provide a 'coarse' evaluation of Ks. For increased sampling precision at lags of 1 and 0.25 m, transects are arranged in pairs oriented both parallel and perpendicular to the toposequence to capture anisotropy in Ks. At 1-m lags, transects are 50 m long and pairs include transects 4 and 5 in the red, clay-rich, upslope areas and transects 6 and 7 in the yellow, sandier, downslope areas. At 0.25 m lags, transects are 20 m long and pairs include transects 8 and 9 and transects 10 and 11. Note that transects 8 and 9 are nested within transects 4 and 5, and transects 10 and 11 are nested within transects 6 and 7. Transect 3 is an additional 50-m transect with lags of 0.25 m at 12.5 and 100 cm depths and lags of 1 m at depths of 20 and 50 cm. The much larger sample size at 12.5 and 100 cm depths along this transect, as compared to sample sizes along the other transects, reveals if sample size is significant for showing spatial structure in Ks.

We took in situ measurements of Ks at depths of 12.5, 20, 50 and 100 cm with an Amoozemeter (Ksat Inc., Raleigh), a compact, constant-head permeameter designed by Amoozegar (1989a). The procedure involved augering a cylindrical hole with radius, r, to the desired depth, establishing a constant head, H, such that $H/r \geq 5$ and monitoring the outflow from the device until a steady-state flow rate is attained; at which point Ks can be calculated via the Glover solution (Amoozegar, 1989b), which considers only the saturated flow component from the auger hole. Measurement attempts in these highly conductive soils sometimes generated outflow that exceeded the instrument's ability to accurately measure this outflow. For these cases, we provided empirically determined, minimum estimates of Ks (500 mm/h for $r = 2$ cm and 300 mm/h for $r = 2.5$ cm) based on results of field experiments.

Our goal was to describe the spatial variability of Ks at the aforementioned scales in these forest soils using different statistical methods. EDA techniques showed these data to be non-Gaussian, so we used the median as a resistant estimator of location with its 95% ($\alpha = 0.05$) confidence interval calculated as follows:

$$\text{Median} \pm \frac{t_{n-1}(d_F)}{1.075\sqrt{n}} \tag{1}$$

where t is the t-statistic at the 95% confidence level for a given sample size, n, and d_F is the fourth spread (Iglewicz, 1983).

In addition to univariate statistics, spatial continuity of Ks was evaluated using geostatistics (i.e. semivariograms). Under the assumption of stationarity, the traditional semivariogram estimator, $\gamma(h)$, was calculated as follows:

$$\gamma(h) = \frac{1}{2N(h)} \left\{ \sum_{i=1}^{N(h)} [Z(x_i + h) - Z(x_i)]^2 \right\} \tag{2}$$

where $N(h)$ is the number of pairs separated by the lag distance, h, and $Z(x_i)$ is Ks measured at spatial locations x_i. S-Plus software was used to generate empirical variograms, and variance is described in these models as: $\gamma(h) = C_o + C_s$. C_o is the nugget variance that occurs at distances smaller than the sampling interval, C_s is the structural variance, and $C_o + C_s$ is the sill (total variance). The range parameter is the distance over

which spatial dependence is apparent for the direction examined. Because of the non-Gaussian distribution of Ks, we also used Eq. (2) on log-transformed data sets. A robust variogram (rodogram) useful for data with outliers proposed by Cressie and Hawkins (1980) is given by:

$$\hat{\gamma}(h) = \frac{\left\{\frac{1}{2N(h)}\sum_{i=1}^{N(h)} /Z(x_i+h) - Z(x_i)/^{1/2}\right\}^4}{0.457 + \frac{0.494}{/N(h)/}} \tag{3}$$

Madograms are also less sensitive to extreme data values and can also be useful for inferring range and anisotropy of data sets with outlier values that may make variogram features difficult to discern using traditional methods. Madograms are similar to traditional variograms except that the absolute difference between $Z(x_i)$ and $Z(x_i+h)$ is calculated rather than the square of the difference. Goovaerts (1997, p. 31) shows the formula as:

$$\gamma M(h) = \frac{1}{2N(h)}\left\{\sum_{i=1}^{N(h)}[/Z(x_i+h) - Z(x_i)/]\right\}, \tag{4}$$

where the notation is the same as for the traditional semivariogram. As a final evaluation of spatial continuity, we used the general relative variogram, which is the traditional variogram in Eq. (2), standardized by the square mean of the data used for each lag. [Goovaerts (1997, p. 85) shows the equation as:

$$\gamma_{GR}(h) = \frac{\gamma(h)}{\left(\frac{m_{+h}+m_{-h}}{2}\right)^2}, \tag{5}$$

where m_{-h} is the mean of $Z(x)$ values and m_{+h} is the mean of $Z(x+h)$ values.

Surveying instruments were used to measure relative topographic variations along transects (Fig. 1) at intervals of 25 m (transect 1) and 1 m (transects 3, 4, 5, 6 and 7), and soil texture and organic matter samples were collected along transects 2, 4 and 6 from the same boreholes used for measuring Ks (Table 1). In addition, we mapped subsurface roots, root pores, other biopores, and loosely consolidated, organic-rich zones that were ≥ 2 mm in diameter. Mapping was conducted along two trenches, each trench 10 m long $\times$ 0.5 m deep, at locations 170–180 and 380–390 m along the toposequence.

Trees represent a central location in space from which root systems emanate and analyzing their spatial patterns may serve as an indicator of subsurface spatial patterns. Consequently, we mapped the spatial point patterns of trees with mean diameter breast height (MDBH) ≥ 2 cm for 20 randomly selected 10×10 m quadrats. For mapped quadrat data, Diggle (1983) recommends the Clark and Evans (1954) significance test for calculating the nearest neighbor distances between trees and testing for complete spatial randomness (CSR). The ratio, R, given by $R = \bar{r}A/\bar{r}E$ equals 1 for a random distribution, and significantly small and large values indicate aggregation and regularity, respectively,

where $\bar{r}A$ represents the mean nearest neighbor distance between trees ($\bar{r}A = \Sigma r/N$) and $\bar{r}E$ represents the mean distance to nearest neighbor expected in an infinitely large random distribution of density rho $\bar{r}E = 1/2\sqrt{\rho}$. The formula used in the test of significance is:

$$c = \frac{\bar{r}A - \bar{r}E}{\sigma\bar{r}E}, \tag{6}$$

where c represents the standard deviate of the normal curve, and $\sigma\bar{r}E$ represents the standard error of the mean distance to nearest neighbor in a randomly distributed population ($\sigma\bar{r}E = 0.26136/\sqrt{N\rho}$).

4. Results

4.1. Spatial patterns of Ks

4.1.1. Univariate statistics

Table 2 lists the upper and lower 95% confidence levels for the median Ks, transect sample size (n) and the percentage of measurement attempts that exceeded the capacity of the instrument (%NM) for each transect. This table is organized so as to compare the median Ks of transects at each depth (12.5, 20, 50 and 100 cm) and sampling scale ($h = 25$, 10, 1 and 0.25 m). These forest soils exhibit a decrease in Ks with depth in which Ks at 12.5 cm, in general, is significantly ($\alpha = 0.05$) greater than Ks at 20 cm depth, which in turn is significantly greater than Ks at 50 and 100 cm depths.

For transects 1 and 2, which span the entire toposequence, there is no significant difference in Ks at the measured depths of 12.5, 20 and 50 cm, indicating that coarse sampling scales of 25 and 10 m capture similar variability in Ks. Significant differences emerge between the shorter transects, however, as the precision of the sampling scale increases to 1 and 0.25 m. The most striking feature of Ks at these sampling scales is that the downslope transects at 20 cm depth (transects 6, 7, 10 and 11) are all significantly greater than those of the upslope transects (transects 3, 4, 5, 8 and 9). The remaining aspects of Table 2 are that there are significant inter- and intra-soil differences in Ks for all other depths and sampling intervals. The percentage of measurement attempts that exceeded the capacity of the instrument (%NM) is highest at depths of 12.5 and 20 cm (2.2–55%), is intermediate at 50 cm depth (0–20%), and is lowest at 100 cm depth (0–4%). Although these measurement attempts could not be factored into the calculation of univariate statistics, their spatial patterns are relevant (discussed next).

4.1.2. Scatter plots of Ks

Fig. 2 shows scatter plots of ‘Ks’ versus ‘distance along toposequence’ for transects 1–11 at the measured depth intervals. At 12.5 cm depth, measurement attempts exceeding the capacity of the instrument are depicted as circles at the top of each scatter plot and are assigned an approximate minimum value of 500 mm/h, whereas those measurement attempts exceeding the capacity of the instrument at 20, 50 and 100 cm depths are depicted as circles with an approximate minimum value of 300 mm/h. Scatter plots for all transects

Table 2
The median Ks value and associated 95% confidence interval for the 11 transects used in this study

Depth (cm)	Transect	Lag (m)	*n*	%NM[1]	LCL[2]	MED	UCL[3]
12.5	1	25	17	5.6	86.5	179.6	272.7
	2	10	44	2.2	166.0	228.3	290.5
	3	0.25	178	20.7	219.9	245.8	271.7
	4	1	42	19.6	135.9	172.2	208.5
	5	1	44	15.4	135.1	168.4	201.7
	6	1	37	27.5	158.1	209.6	261.1
	7	1	41	21.2	164.3	239.5	314.7
	8	0.25	71	12.5	102.8	134.7	166.6
	9	0.25	54	31.6	185.1	232	278.9
	10	0.25	59	23.5	235.8	269.4	303.0
	11	0.25	73	6.4	112.3	149.7	187.1
20	1	25	17	5.6	30.1	67.5	104.9
	2	10	43	4.4	21.3	33	44.7
	3	1	35	20.0	4.0	30.3[B]	56.6
	4	1	39	22.0	25.3	36.6[B]	47.9
	5	1	45	11.8	13.3	17.4[B]	21.5
	6	1	31	36.7	78.0	109.9[A]	141.8
	7	1	23	54.9	92.8	139.2[A]	185.6
	8	0.25	76	5.0	17.3	20.9[B]	24.5
	9	0.25	72	8.9	23.7	30[B]	36.3
	10	0.25	78	12.8	99.0	109.9[A]	120.8
	11	0.25	64	17.9	91.1	102.6[A]	114.1
50	1	25	18	0.0	− 4.5	11.0	26.5
	2	10	45	0.0	1.6	4.1	6.6
	3	1	43	10.2	9.1	14.6	20.1
	4	1	49	2.0	15.6	21.9	28.2
	5	1	48	4.0	3.8	7.6	11.4
	6	1	38	12.2	− 5.5	17.6	40.7
	7	1	40	20.0	21.9	36.9	51.9
	8	0.25	77	3.8	23.8	28.5	33.2
	9	0.25	73	6.4	38.1	47.6	57.1
	10	0.25	75	0.1	9.8	11.9	14.0
	11	0.25	74	2.6	26.6	32.1	37.6
100	3	0.25	194	1.5	37.6	42.5	47.4
	4	1	48	2.0	20.6	32.2	43.8
	5	1	48	4.0	9.4	13.5	17.6
	6	1	47	0.0	13.1	22.7	32.3
	7	1	46	2.2	32.3	44.7	57.1
	8	0.25	72	2.7	11.7	14.7	17.7
	9	0.25	76	2.6	12.8	19.9	27.0
	10	0.25	73	0.0	6.0	7	8.0
	11	0.25	73	0.0	6.4	10.5	14.6

Median Ks for ‘A’ is significantly higher than median Ks for ‘B’.

[1] This indicates percentage of Ks measurement attempts that exceeded capacity of instrument.

[2] This represents lower 95% confidence level.

[3] This represents upper 95% confidence level.

show high values commonly followed by low values with few obvious spatial trends. At 12.5 cm, there are small clusters of high Ks values for some transects at short lags (transect 6 from 378 to 401; transect 7 from 14 to 28; transect 8 from 168 to 169, 174.5 to 175.5; transect 9 from 0 to 2.5, 9 to 13). In addition, transects 6 and 7 show clearly defined high Ks zones. For transect 6, these occur from 375 to 401 m (20 cm depth), 384 to 401 (50 cm depth) and 391 to 401 (100 cm depth). For transect 7, the high Ks zones occur at − 18 to 3 and 17 to 25 m (20 cm depth) and are only weakly defined at 50 cm depth.

4.1.3. Semivariograms of Ks

Fig. 3 shows semivariograms of Ks for transect 3 using the following methods: traditional semivariograms on untransformed and log-transformed Ks, rodograms, mado-

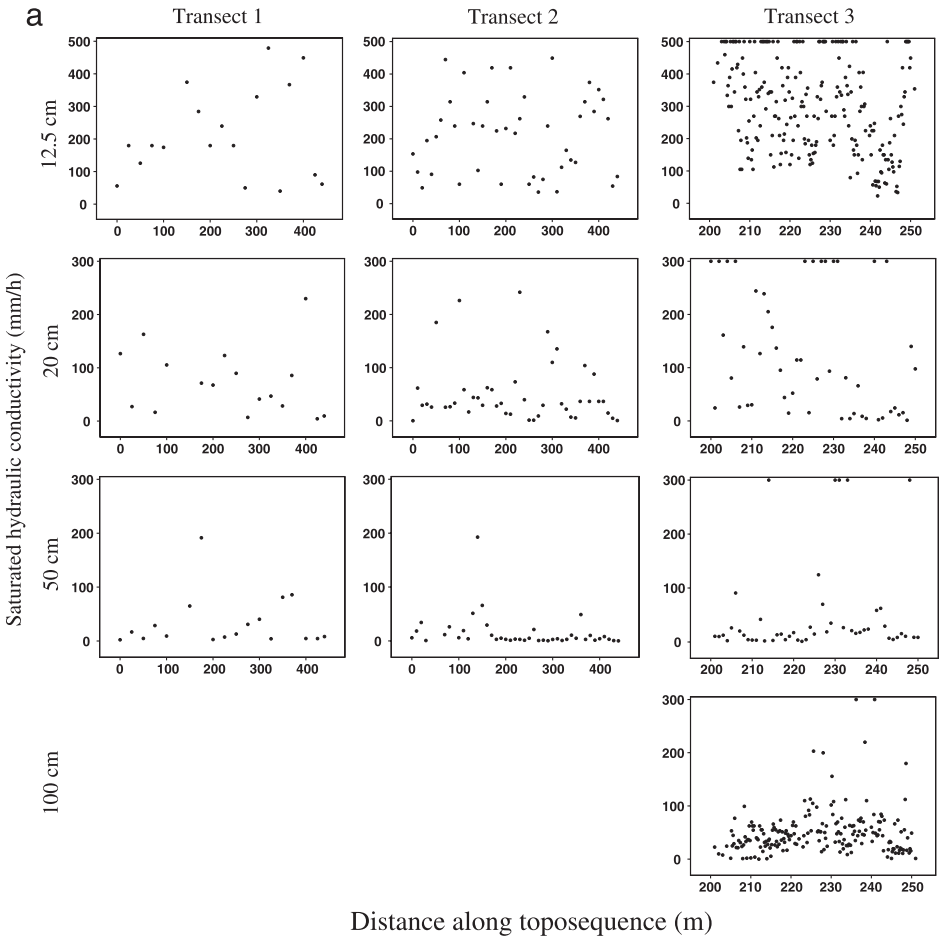

Fig. 2. Scatter plots of 'Ks' versus 'Distance along toposequence' at measured depth intervals for (a) transects 1–3, (b) transects 4–7, and (c) transects 8–11.

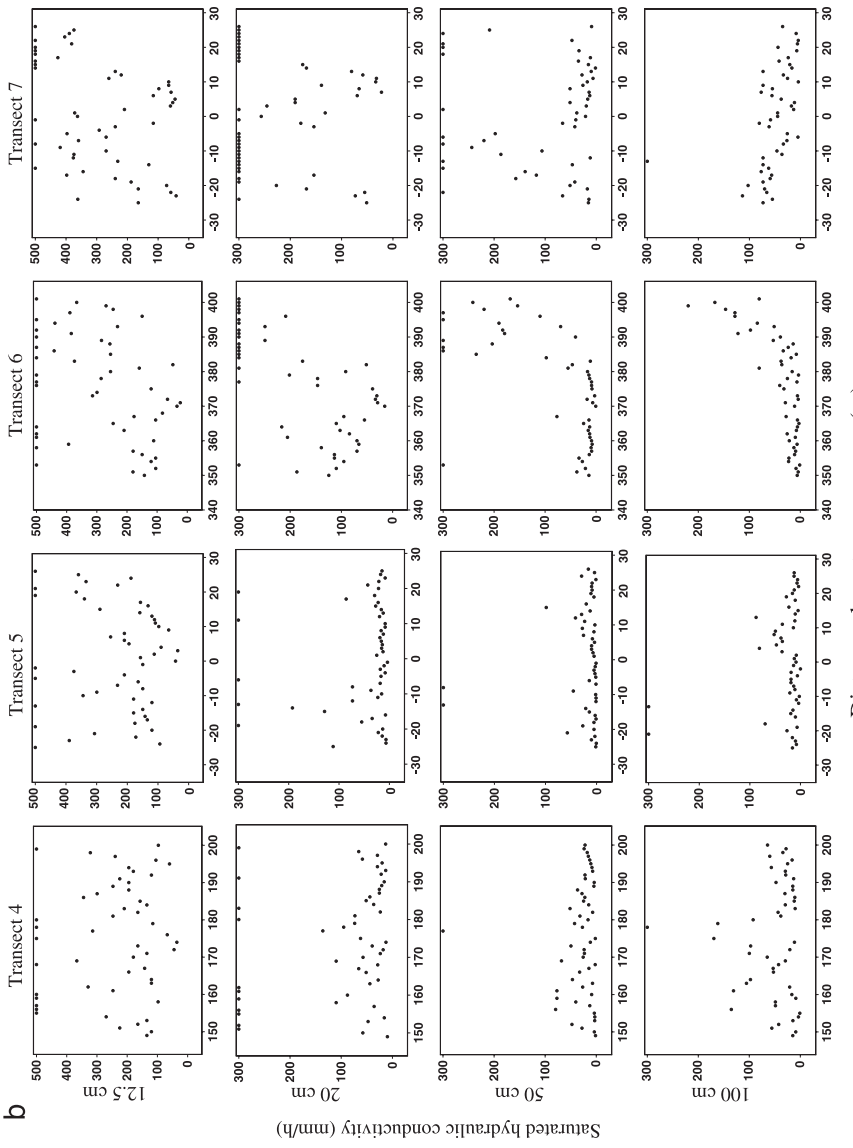

Fig. 2 (*continued*).

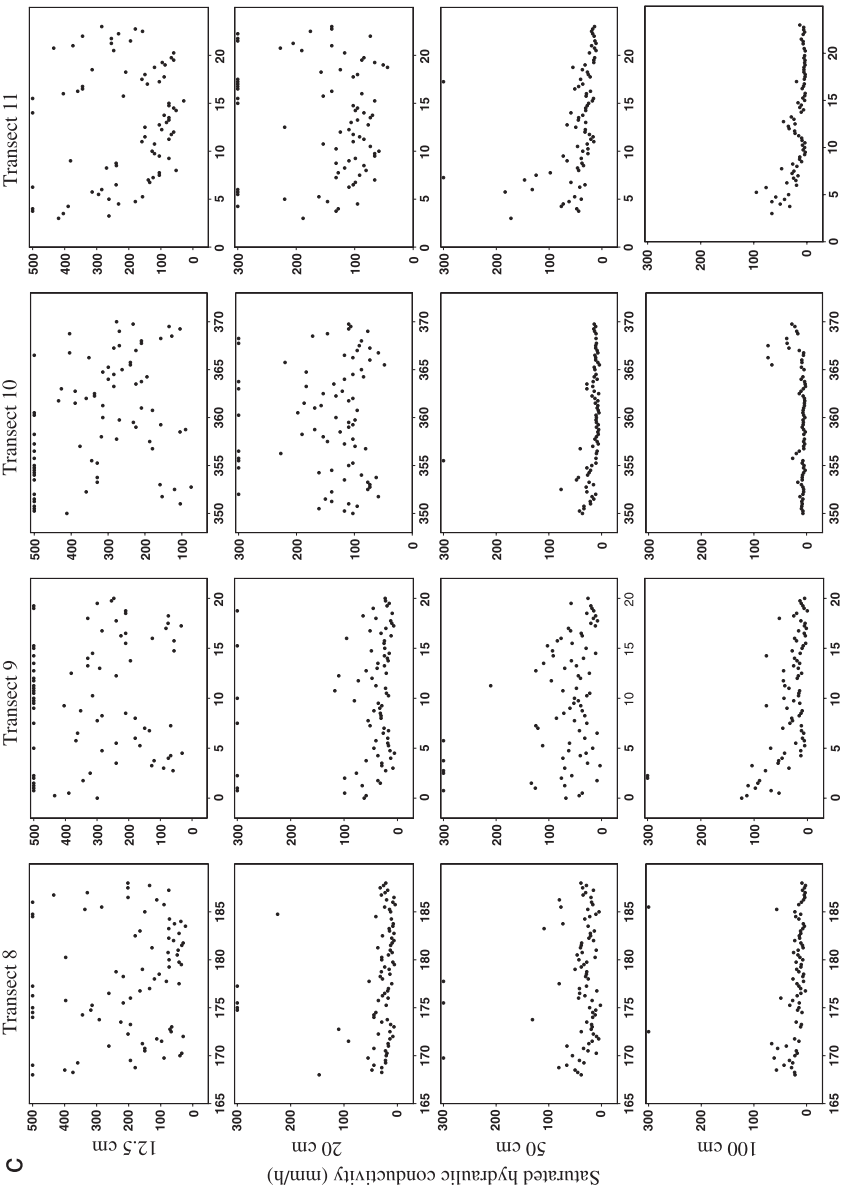

Fig. 2 (*continued*).

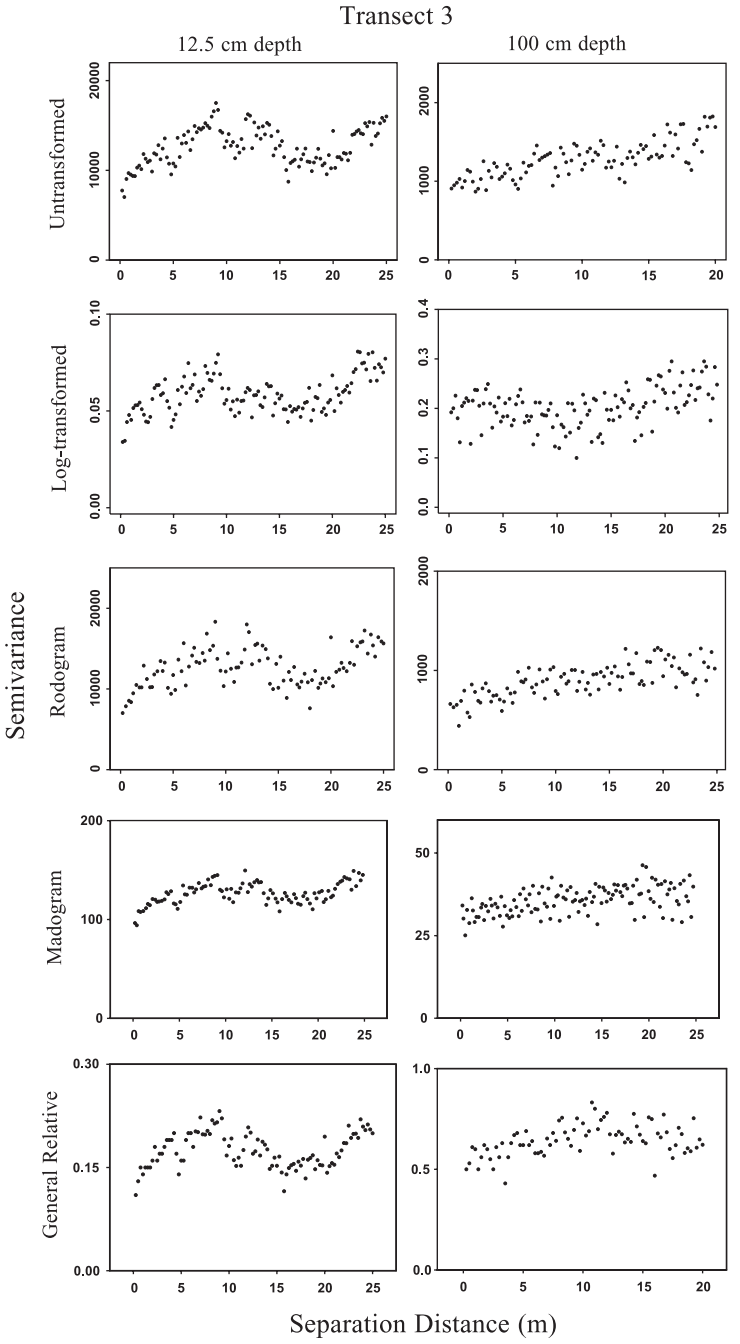

Fig. 3. Semivariograms of Ks for transect 3 using various methods of estimating semivariance including semivariograms on untransformed data, semivariograms on log-transformed data, rodograms, madograms and general relative variograms.

grams and general relative variograms. It is evident in Fig. 3 that spatial continuity of Ks is similarly represented by all types of semivariograms for transect 3, as well as all other transects (not shown), so only traditional semivariograms are presented for the remainder of the transects (Fig. 4a–c). Because this study investigates the relationship between structural and nugget variance at different sampling scales, the *y*-axis (semivariance) is uniform for all transects at a given depth interval, thus allowing an easier comparison of the magnitude of variability between transects. In addition, semivariograms are presented so that the paired transects at different scales are next to each other; i.e. semivariograms for transects 4 and 5 ($h = 1$ m) are next to those of transects 8 and 9 ($h = 0.25$ m), and semivariograms for transects 6 and 7 ($h = 1$ m) are next to those of transects 10 and 11 ($h = 0.25$ m).

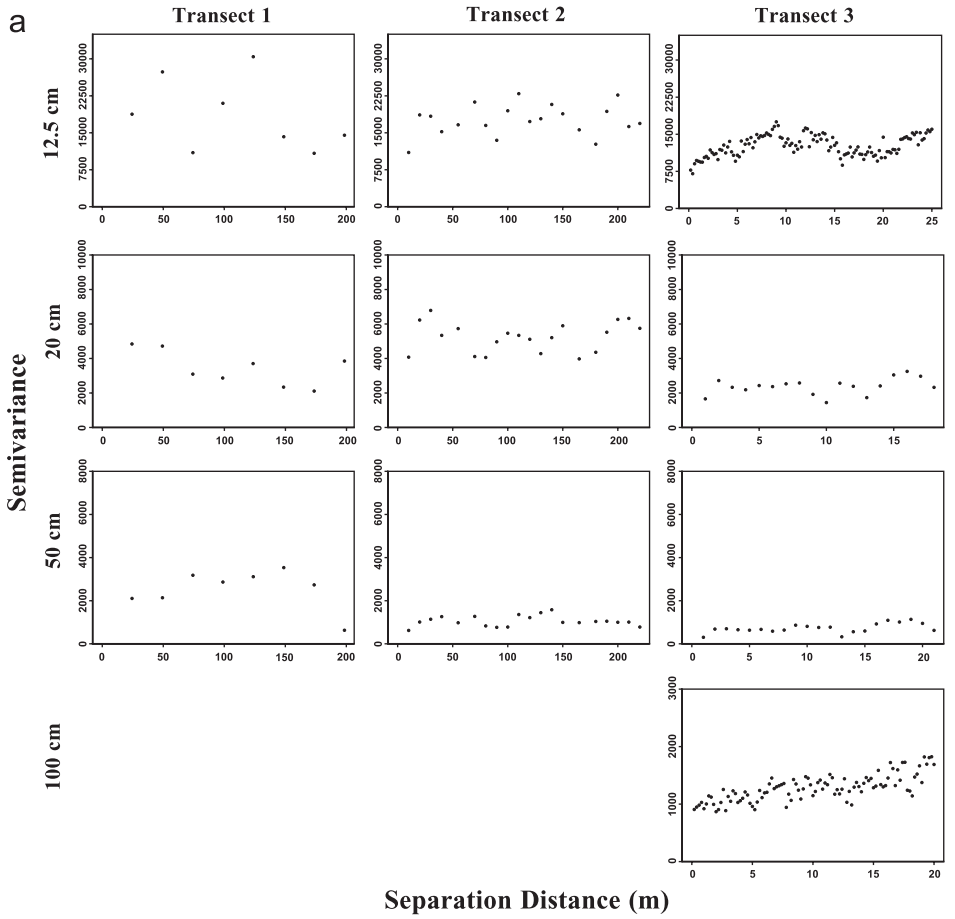

Fig. 4. Semivariograms of Ks at the various depth intervals for (a) transects 1–3, (b) transects 4, 5, 8 and 9, and (c) transects 6, 7, 10 and 11.

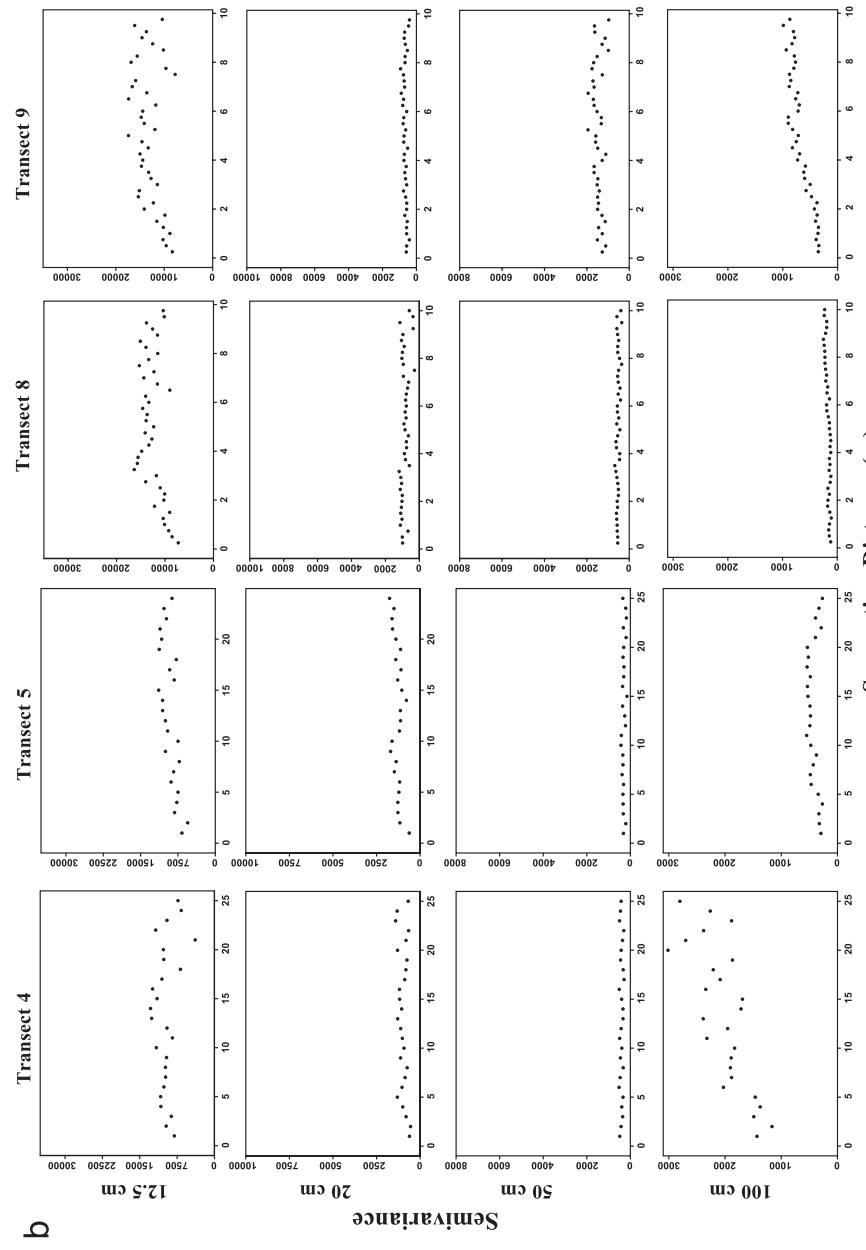

Fig. 4 (*continued*).

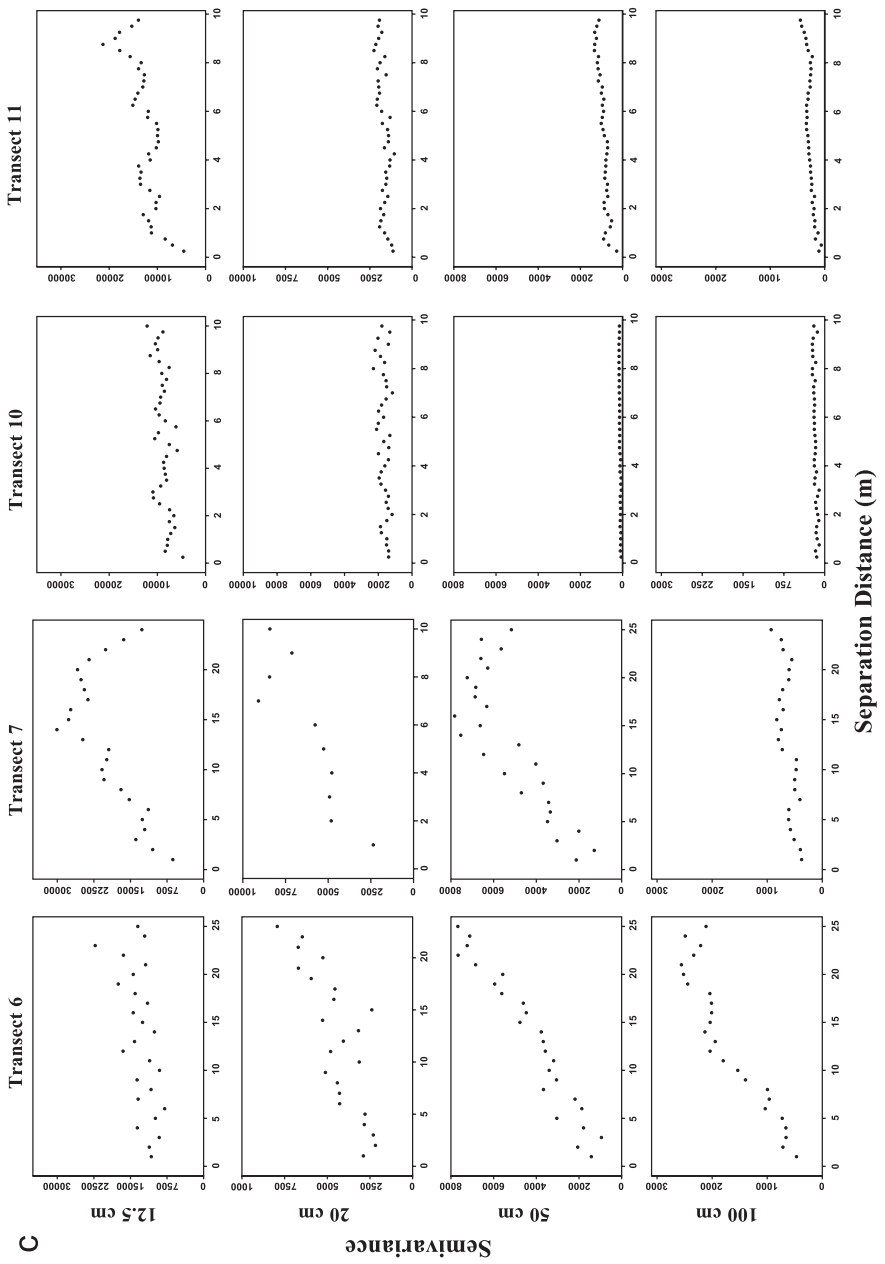

Fig. 4 (*continued*).

Transects 1 and 2 are designed to reveal if spatial structure in Ks emerges from noise at the catena-wide scale as sampling precision increases from 25 m (transect 1) to 10 m (transect 2). Empirical variograms for both transects show no apparent spatial structure and have similar sill values, suggesting no reduction in the variability of Ks. An exception occurs at 50 cm depth where transect 2 has a lower sill and nugget with a range <50 m.

Semivariograms of Ks for paired transects in the upslope, clay-rich locations (transects 4, 5, 8 and 9) show remarkable similarity in sill values and in their general lack of spatial structure at both sampling scales of 1 and 0.25 m. The notable exception occurs for transect 4 at 100 cm depth, which has a larger nugget and sill and a range of approximately

Table 3
Summary statistics for percentages of sand, silt, clay and organic matter (g/kg)

ID	Depth (cm)	Property	Mean	S.D.	*n*
Transect 2	0–12.5	%Sand	73.6	9.6	45
		%Silt	5.0	1.6	45
		%Clay	21.4	8.6	45
		Organic matter	21.8	14.0	45
	12.5–20	Sand	68.0	10.2	45
		Silt	7.2	2.1	45
		Clay	24.7	8.6	45
		Organic matter	13.2	7.6	45
	40–50	Sand	61.4	10.6	41
		Silt	8.4	4.5	41
		Clay	30.2	7.5	41
		Organic matter	7.8	2.3	41
Transect 4	0–12.5	Sand	65.8	3.4	50
		Silt	7.0	1.6	50
		Clay	27.2	2.5	50
		Organic matter	23.7	12.2	50
	40–50	Sand	58.5	2.1	49
		Silt	8.0	1.4	49
		Clay	33.4	1.6	49
		Organic matter	6.9	2.7	49
	90–100	Sand	54.5	2.3	48
		Silt	8.5	1.6	48
		Clay	37.0	2.6	48
		Organic matter	6.4	2.1	48
Transect 6	0–12.5	Sand	83.4	4.1	51
		Silt	4.9	2.0	51
		Clay	11.7	3.3	51
		Organic matter	18.7	5.0	51
	40–50	Sand	73.9	6.9	51
		Silt	6.2	2.1	51
		Clay	19.9	6.6	51
		Organic matter	11.0	2.1	51
	90–100	Sand	63.3	9.0	51
		Silt	7.1	2.2	51
		Clay	29.6	7.8	51
		Organic matter	9.8	2.2	51

15 m. Semivariograms for transect 3 in the upslope, clay-rich area, are similar to those of transects 4, 5, 8 and 9, despite having much larger sample sizes at the 12.5 and 100 cm depth intervals. There is an approximately 2–3 m cyclicity at the 12.5 cm depth interval (Figs. 3 and 4a).

Semivariograms of transects in the downslope, sand-rich locations (transects 6, 7, 10 and 11) are considerably different and exhibit more anisotropy than those in the upslope areas. All of these semivariograms have a relatively small proportion of nugget variance, but the sill values are much larger and nugget values only slightly larger for transects 6 and 7 ($h = 1$ m) than for transects 10 and 11 ($h = 0.25$) at all depth intervals. At 12.5 cm depth, variograms for transects 10 and 11 exhibit an approximately 2 m cyclicity similar to that of transect 3.

4.2. Spatial patterns of physical properties

In Section 4.1, we characterize spatial patterns in Ks as a function of sampling scale across the entire toposequence and between upslope and downslope areas. This section evaluates scale dependency in spatial patterns of selected soil properties including texture, organic matter and biological features.

4.2.1. Soil texture

Soil samples for percentages of sand, silt and clay (%SSC) were collected at 10 m intervals along the entire toposequence and at 1 m intervals from locations 150–200 and 350–400 m (Fig. 1, transects 2, 4 and 6, respectively). Table 3 lists the univariate statistics for these properties, and Table 4 lists the general textural classes for samples. The catena-wide textural variability (sandy clay to sand) is captured by transect 2, which shows a predominance of sandy clay loam and sandy loam from 0 to 12.5 cm depth replaced by sandy clay and sandy clay loam by 40–50 cm depth. For transect 4, there is little variability in textural classes (i.e. sandy clay loam and sandy clay) at the sampled depths of 0–12.5, 40–50 and 90–100 cm. Transect 6 shows considerable variability in texture with a predominance of sandy loam and loamy sand at 0–12.5 cm depth replaced by sandy clay and sandy clay loam at 90–100 cm depth.

Scatter plots for the %SSC along transect 2 reveal distinctive spatial patterns at the measured depths of 0–12.5 and 40–50 cm showing a downslope increase in sand,

Table 4
Percentage of soil samples in each textural class

ID	Depth (cm)	Sandy clay	Sandy clay loam	Clay loam	Sandy loam	Loamy sand	Sand
Transect 2	0–12.5	4.3	53.2	0.0	22.6	15.5	4.3
	40–50	31.7	56.1	2.4	7.3	2.4	0.0
Transect 4	0–12.5	0.0	100.0	0.0	0.0	0.0	0.0
	40–50	14.3	85.7	0.0	0.0	0.0	0.0
	90–100	64.6	35.4	0.0	0.0	0.0	0.0
Transect 6	0–12.5	0.0	0.0	0.0	41.2	43.1	15.7
	40–50	0.0	58.8	0.0	17.6	23.6	0.0
	90–100	33.3	56.9	0.0	9.8	0.0	0.0

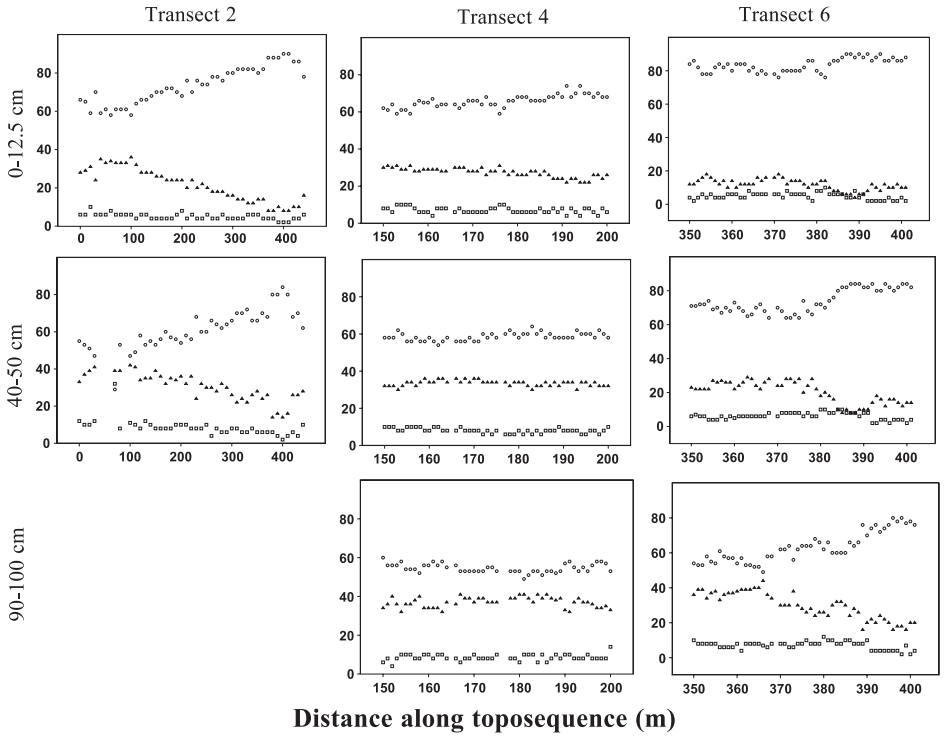

Fig. 5. Scatter plots showing the percentages of sand (open circle), silt (open square) and clay (solid triangle) from soil samples along transects 2, 4 and 6 at various depths.

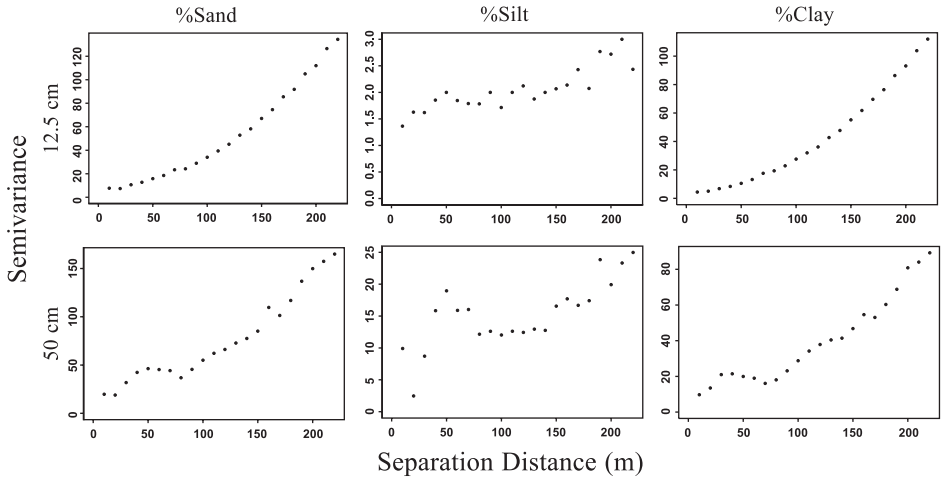

Fig. 6. Semivariograms for percentages of sand, silt and clay for transect 2.

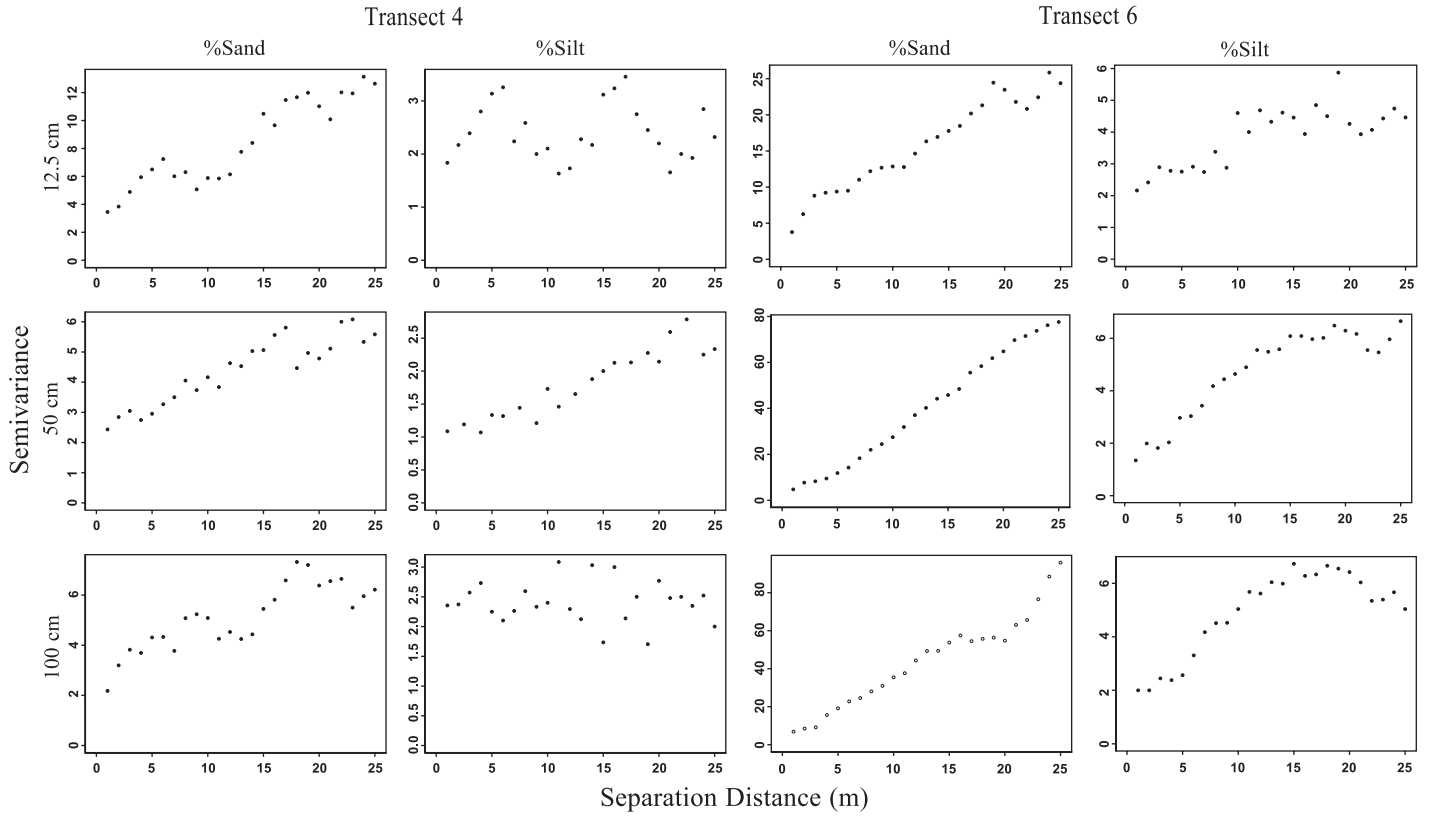

Fig. 7. Semivariograms for percentages of sand and silt for transects 4 and 6.

decrease in clay, and little variation in silt (Fig. 5). For transect 4 in the upslope areas of the catena, scatter plots show no obvious textural trends with the exception of a gentle downslope increase in sand and decrease in clay at 0–12.5 cm depth. For transect 6 in the downslope areas, scatter plots at all three depths show abrupt, step-like increases in sand and decreases in clay with little variation in silt. These 'steps' occur at approximately 384 m (0–12.5 cm depth), 388 m (40–50 cm depth), and 368 and 388 m (90–100 cm depth) along the toposequence.

Empirical variograms of %SSC show ranges exceeding the scale of observation (>220 m) for transect 2 (Fig. 6), reflecting the large-scale, catena-wide spatial patterns of these properties evident in the scatter plots. Empirical variograms for transect 4 (Fig. 7) show variogram ranges ≥ 15 m for sand and clay (semivariograms for %sand and %clay are similar so only those of %sand are shown) with a relatively small component of nugget variance at all depths. Variograms for silt show a large nugget with an ~ 10 m cyclicity at 0–12.5 cm depth, a range of ~ 20 m, and little nugget variance at 40–50 cm but show complete nugget variance at 90–100 cm. For transect 6 (Fig. 7), empirical variograms of sand, silt and clay show spatial structure ≥ 15 m with little to no apparent nugget variance.

4.2.2. Organic matter

The concentrations of organic matter are presented in Table 3. For all transects, the concentrations of organic matter are highest at the 0–12.5 cm interval with mean values of

Table 5
Percentage area and counts (in parentheses) of features ≥ 2 mm in diameter including biopores, roots, and loosely consolidated, organic-rich zones exposed in cross section along trenches

Depth (m)	Biopores	Roots	Organic zones	Total (%)
10 × 0.5 m trench 170–180 m along toposequence				
0–0.05	0.24 (1)	0.48 (28)	3.38 (4)	4.10
0.05–0.10	2.15 (2)	0.59 (28)	3.54 (4)	6.28
0.10–0.15	1.72 (2)	0.25 (13)	1.00 (1)	2.97
0.15–0.20	0.76 (4)	0.05 (9)	0.00	0.81
0.20–0.25	2.89 (9)	0.03 (6)	0.00	2.92
0.25–0.30	2.14 (2)	0.09 (10)	0.00	2.23
0.30–0.35	1.95 (5)	0.13 (11)	0.00	2.08
0.35–0.40	3.25 (7)	0.08 (9)	0.00	3.33
0.40–0.45	2.97 (3)	0.01 (3)	0.00	2.98
0.45–0.50	1.40 (3)	0.03 (3)	0.00	1.43
10 × 0.5 m trench 380–390 m along toposequence				
0–0.05	0.02 (2)	1.62 (41)	2.56 (2)	4.20
0.05–0.10	2.9 (4)	5.62 (49)	1.80 (2)	10.31
0.10–0.15	1.26 (8)	1.27 (21)	2.12 (1)	4.65
0.15–0.20	0.40 (7)	0.51 (22)	2.08 (1)	2.99
0.20–0.25	0.85 (11)	0.95 (22)	1.92 (1)	3.72
0.25–0.30	0.41 (8)	0.18 (12)	1.28 (1)	1.87
0.30–0.35	0.39 (8)	0.22 (19)	0.00	0.61
0.35–0.40	0.31 (5)	0.36 (15)	0.00	0.67
0.40–0.45	0.60 (7)	0.26 (13)	0.00	0.86
0.45–0.50	0.04 (6)	0.04 (5)	0.00	0.08

21.8 (transect 2), 23.7 (transect 4) and 18.7 (transect 6) g/kg. At the 40–50 cm depth interval, mean organic matter concentrations range from 6.9 to 11.0 g/kg, and concentrations range from 6.4 to 9.8 g/kg at 90–100 cm.

4.2.3. Biological features

Table 5 shows counts and the percentage area of biopores, roots and loosely consolidated organic zones ≥2 mm in diameter identified in soils within each of the two trenches and tabulated at 5 cm depth intervals. The most important aspect is that there is a relatively high total percentage of biological features (biopores + roots + organic zones) at any given soil depth, which always exceeds 0.6%. The total cross-sectional area of these features is generally highest within the uppermost 15 cm (2.97–10.31%) of these soils. Soils from the trench at 380–390 m show a sudden drop (<0.9%) in the percentage area

Table 6
Results of nearest neighbor analysis of spatial point patterns of trees with varying mean diameter breast heights (MDBH) from mapped quadrat data

100-m^2 Quadrat	Trees ≥2 cm MDBH		Trees ≥3 cm MDBH		Trees ≥4 cm MDBH		Trees ≥5 cm MDBH	
	Count	NN distance (m)	Count	NN distance (m)	Count	NN distance (m)	Count	NN distance (m)
1	27	1.30***	26	1.33***	19	1.58***	16	1.82***
2	30	1.11**	22	1.31*	19	1.50**	12	1.63
3	25	1.23*	18	1.34	16	1.45	15	1.56
4	25	0.96	19	1.20	15	1.32	14	1.36
5	28	1.03	24	1.06	19	1.21	18	1.29
6[a]	15	1.76**	10	2.06	9	2.52**	9	2.52**
7	36	0.79	25	0.91	18	1.13	14	1.63
8	29	1.04	22	1.31*	18	1.35	14	1.65
9	31	1.08**	20	1.26	18	1.30	17	1.26
10	30	1.18***	25	1.21*	23	1.25*	20	1.22
11	37	0.99**	31	1.15***	26	1.37***	17	1.64***
12	28	1.09	21	1.40*	18	1.41	15	1.38
13	26	1.04	17	1.18	13	1.72	9	2.67***
14	26	0.94	19	1.16	16	1.37	13	1.40
15	31	0.79	26	1.00	19	1.24	14	1.37
16	31	1.02	22	1.26	19	1.52**	14	1.82**
17	27	0.91	18	1.15	12	1.55	10	2.05
18	22	1.09	17	1.44	14	1.64	12	1.82
19	28	1.09	19	1.31	13	1.69	13	1.97**
20	27	0.94	21	1.42**	17	1.64**	12	1.88*

[a] Counts in this quadrat suspect because a large path crosscuts area.

* This indicates 90% probabilities of a greater difference between measured and an infinitely large random distribution of nearest neighbor distances for regularity.

** This indicates 95% probabilities of a greater difference between measured and an infinitely large random distribution of nearest neighbor distances for regularity.

*** This indicates 99% probabilities of a greater difference between measured and an infinitely large random distribution of nearest neighbor distances for regularity.

of all features at depths greater than 30 cm, whereas this is not the case for the trench from 170 to 180 m, in which features range between 1.43% and 3.33% at depths between 30 and 50 cm. Other differences in counted features between trenches are that large burrows are more common in the 170–180 m trench, as reflected in the low counts but large percentage area biopores from 5 to 15, 25 to 30, and 40 to 50 cm depths, but roots are more common and areally extensive in the 380–390 m trench. Because root systems and burrows are ubiquitous throughout the toposequence, we do not suggest that the differences in biological features observed in two trenches reflect spatial patterns within different soil types along this catena.

Table 6 shows the results of nearest neighbor analysis for spatial point patterns of trees within 100-m^2 quadrats. The nearest neighbor distances are generally between 1–2 m, and the distances become shorter as the mean diameter breast height is decreased. Significance tests show that tree patterns are not significantly different from complete spatial randomness (CSR) for most quadrats, but some quadrats show significant departures from CSR for regularity.

5. Discussion

5.1. Linking spatial patterns of hydraulic and physical properties

Catena-wide spatial patterns are clearly evident for topography and soil textural components, as reflected in scatter plots. Ks scatter plots, however, show considerable noise and little to no spatial structure at the coarsest sampling scales of 25 and 10 m. These contrasting results suggest no link between Ks and these physical properties at coarse sampling scales. As sampling precision increases to 1 m, scatter plots of Ks reveal clear spatial patterns along transects 6 and 7, consisting of hydraulic boundaries separating high versus low Ks zones at multiple depths (Fig. 2b). These spatial patterns of Ks correspond remarkably well to the textural and topographic data for transect 6 (there are no texture data for transect 7). The topographic profile for transect 6 shows two downslope steps occurring at locations 362 and 384 m along the toposequence (Fig. 1). Texture scatter plots show step-like increases (%sand) and decreases (%clay) at location 384 m for depths of 12.5 and 50 cm and at locations 384 and 365 m at 100 cm depth (Fig. 4), and it is this tight link between textural and topographic features that defines a toposequence. Hydraulic zones of Ks, however, only correspond to the topographic step at location 384 m on the toposequence.

Why does this hydraulic boundary occur for one topographic/texture step and not the other? Texture scatter plots for transect 6 show that the high Ks zone occurs only in those locations where the concentration of sand $\geq 80\%$ and clay $\leq 20\%$, suggesting that very coarse textures (loamy sand and sand) are influential in controlling Ks. McKeague et al. (1982, p. 1240) evaluated Ks from 38 sites and 78 soil horizons and found Ks values to range between 167 and 500 mm/h for soils with a ‘texture of fine sand with very little finer material or of loamy medium or coarser sand, friable, not compressed’, and Ks was >500 mm/h for soils with ‘texture coarser than fine sand, friable, no strata or finer material’. Our coarse textures along transect 6 likely occur within the informal textural description of

McKeague et al. (1982) and, therefore, it is not surprising that our Ks values occur within a similar range.

The idea of whether extremely coarse textures influence spatial patterns of Ks is further supported by reviewing the data from transect 4, consisting of relatively fine-grained soils with little variation. Neither scatter plots of Ks nor those for textural components show any apparent spatial patterns. Transect 7, which occurs in close proximity to transect 6, has multiple high Ks zones at depths of 12.5, 20 and 50 cm. In the absence of soil textural data, however, we can only surmise that these zones correspond to texturally coarse areas. Spatial patterns of Ks along transect 6 (and likely transect 7) appear to be controlled by intrinsic factors (e.g. pore size distribution and soil type) rather than extrinsic factors (e.g. root growth and decay, burrows) with these terms being defined by Mohanty et al. (1994, p. 2490). Using the terminology of Ringrose-Voase (1991), structural pore space (mineralogy-related) rather than nonstructural pore space (bioturbation-related) is the dominant controlling factor of Ks along transect 6.

5.2. Structure versus noise

Although scatter plots are useful in showing spatial patterns between variables, semivariograms are quantitative tools for evaluating spatial continuity by showing the proportion of structural variance and the range of autocorrelation. In addition, there are different positions as to what a semivariogram represents with extreme positions being: (1) variogram is not dependent on the data but rather is introduced based on other information, and (2) variogram is estimated only from the data (Kitanidis, 1997, p. 84). These positions become relevant for this study because catena-wide spatial patterns of soil physical properties generate an expectation for the spatial patterns of Ks, thus favoring the former position.

Our results show little to no spatial structure in Ks for semivariograms at lags of 25 and 10 m, whereas those for soil physical properties reflect large-scale, catena-wide spatial structure. These results suggest no link between Ks and the properties of %SSC. Furthermore, these results suggest that if there is spatial structure in Ks, then it emerges at smaller sampling scales, i.e. at lags <10 m, and it must be caused by processes operating at these scales.

Semivariograms of Ks in the upslope, clay-rich locations (transects 3, 4, 5, 8 and 9) are statistically interesting. Based on the two criteria for evaluating spatial continuity (i.e. proportion of structural variance and range), semivariograms at all scales ($h=1$ and 0.25 m) generally show little to no spatial structure. With the exception of semivariograms at 100 cm, the sill and nugget values are fairly similar between these transects. Semivariograms of textural components (%SSC) along transect 4 typically show ranges between 5 and 25 m and a high proportion of structural variance. These findings suggest no link between the spatial patterns of Ks and soil texture at these sampling scales along this part of the catena and further support the predominance of small-scale processes for influencing Ks.

Semivariograms for the downslope, sand-rich areas (transects 6, 7, 10 and 11) reveal spatial structure in Ks and show lower nugget and sill values with increasing sampling

precision. Semivariograms of soil physical properties and Ks along transect 6 show many similarities. For example, semivariograms of Ks, %sand and %clay at 50 and 100 cm depths all show little nugget variance and a range that exceeds 25 m. Significant differences occur at 12.5 cm depth, however, where variograms of Ks are noisy but those of sand and clay still exhibit spatial structure. Because scatter plots of Ks and sandy textures show similar spatial patterns at 50 and 100 cm depths, the similarity of semivariograms between these features at these depths is not surprising. The lack of similarity in spatial patterns at 12.5 cm depth is addressed next.

5.3. Suggested role of biological activity

The previous sections show that Ks has little to no spatial structure along this toposequence except where there are extremely coarse textures. Although the link between coarse textures and Ks is evident at depth intervals of 20, 50 and 100 cm for transect 6, the link is not as apparent at 12.5 cm where spatial patterns of Ks are expected to be strongest because textures are coarsest. Table 2 shows that median Ks values of the sand-rich transects along transects 6, 7, 10 and 11 are all significantly ($\alpha = 0.05$) greater than those of transects 3, 4, 5, 8 and 9 at 20 cm depth. Why is not Ks also significantly greater at 12.5 cm depth where the textural contrasts are even more pronounced? In addition, why is Ks for all transects highest at 12.5 cm depth, but there is commonly no significant difference between soil types at this depth? Finally, why is there consistently little to no spatial structure in semivariograms at 12.5 cm depth, irrespective of location along the toposequence?

We suggest that numerous, small-scale biological processes are generating macropores (extrinsic factors of Mohanty et al., 1994; nonstructural porosity of Ringrose-Voase, 1991) that override the effect of coarse textures on Ks near the soil surface. This is supported by the largest percentage of roots, biopores and loosely consolidated, organic-rich zones occurring within the uppermost 15 cm of these forest soils. The number of measurement attempts exceeding the capacity of the instrument (%NM) is greatest at 12.5 and 20 cm depths, which is likely a result of soil macroporosity associated with the biological features. The highest concentration of organic matter at 12.5 cm also supports biological activity as the cause of these spatial patterns of Ks, because organic matter serves as an indicator of plant and animal activity. In addition, the nearest neighbor distance of trees is typically less than 2 m, and this value may serve as a minimum estimate of spatial distances between subsurface root systems that influence Ks.

Even though we suggest that these small-scale biological processes are making Ks noisy even at sampling scales of 1 and 0.25 m, it is also possible that they are creating small-scale spatial patterns. Semivariograms of Ks along transects 3, 10 and 11 at 12.5 cm depth at lags of 0.25 m show approximately 2 m cyclical rise and fall patterns. We speculate that nearest neighbor distances of trees (1–2 m) and their regularity in space (i.e. departure from complete spatial randomness) in some locations are causing the $\sim$ 2 m cyclical patterns observed in Ks for transects 3, 10 and 11. This speculation cannot be proven, but Mallants et al. (1997) offered a similar speculation for a 4-m cycle observed in Ks for their soils.

5.4. Comparison of published Ks spatial structure studies

Table 7 shows published studies on the spatial structure of Ks, and these studies have differences in soil type, land use, depth interval, measurement method and lag interval. An inter-study comparison shows semivariogram ranges for Ks between 0 and 115 m and nugget variances between 6% and 100%. For studies of agricultural soils, Tsegaye and Hill (1998) and Bosch and West (1998) suggest tillage practices are the cause for higher nugget variances at the shallowest depths, and Mohanty and Mousli (2000, p. 3321) included the effects of traffic, roots, worms, and freezing/thawing cycles, in addition to tillage, as causes for these higher nugget variances at shallow depths. Mallants et al. (1996, p. 176) found lower nugget variances and longer ranges of correlation in Ks at shallow depths, which they attributed to higher biological activity. Sobieraj et al. (2002) found no spatial structure along a tropical rainforest catena at lags of 25 m and speculated that biological processes were generating macropores overriding significant soil textural differences at this scale. This study, which occurs over the same catena, confirms that there is generally little to no spatial structure for these soils at lags of 25, 10, 1 and 0.25 m, except where there are extremely coarse textures. In addition, Lauren et al. (1988) and Mallants et al. (1997) found spatial correlation between Ks and macropore area, and the former study also found Ks to be correlated with percentages of silt and clay. Finally, some studies (Ciollaro and Romano, 1995; Wilson and Luxmoore, 1988; Wilson et al., 1989) describe spatial structure in Ks but offer no explanation as to the underlying cause.

5.5. Necessity for multi-scale spatial studies

This study underscores the importance of conducting multi-scale investigations because we show, for example, that intrinsic and extrinsic factors control spatial patterns of Ks, but these relationships are only apparent at some scales but not at others. A simple study at a single scale would fail to capture these results. Litaor et al. (2002) conducted a multi-scale study on the spatial structure of soil color, texture, organic C, pH, bulk density, and soil moisture along an alpine tundra catenary sequence in Colorado. Their results suggested that micro-scale variations in alpine soils resulted from the effects of cryoturbation, biological activity, parent-material and eolian deposition, but large-scale variations were attributed to the topographic/snow gradient. In their study, Litaor et al. (2002) argue that a lack of spatial structure in soil texture was explained, at least in part, by biological processes masking the expected long-distance variations of their 550-m catena. Interestingly, we argue the biological processes are masking potential long-distance variations of Ks but not actual variations of soil texture.

Oline and Grant (2002) conducted a multi-scale ecological investigation of soil water content, organic matter, pH, and total soil biomass over a 22-km distance ranging from dry forested foothills to alpine tundra in Colorado. They argue that because biological communities simultaneously respond to multiple variables with differing patterns of spatial variation, the spatial variation of these communities will be at least as complex as the most complex environmental variable for a given site. For our study, we attribute the

Table 7
Published studies on spatial structure of Ks

Study	Soil/land use	Depth (m)	Method	Lag (m)	Range (m)	%Nugget
Bosch and West (1998)	Pine flat (PF) soil series and Troup soil series in tilled field near Plains, GA	0.25, 0.5, 1.4, 2.0	In situ with constant-head permeameter	5	PF: 0.25 (4.9 m), 0.5 (2.0 m), 1.4 (17 m), 2 (26 m); Troupe: 0.25 (37.5 m), 0.5 (98.7 m), 1.4 (115.3 m), 2 (16.4 m)	PF: 0.25 (46%), 0.5 (96%), 1.4 (17.6%), 2 (7%); Troupe: 0.25 (62%), 0.5 (6%), 1.4 (15%), 2 (67%)
Ciollaro and Romano (1995)	Volcanic Vesuvian soil in agricultural area	0.45	Lab method on 0.0003-m^3 cores	1	0.45 (6 m)	0.45 (15%)
Lauren et al. (1988)	Glossaquic Hapludalf, argillic horizon near Cornell University campus	0.3	Lab method on 0.12-m^3 and 0.05-m^3 cores	10	0.12 m^3 (60 m), 0.05 m^3 (80 m)	0.12 m^3 (<10%), 0.05 m^3 (50%)
Mallants et al. (1996)	Udifluvent in orchard near Leuven, Belgium	0.1, 0.5, 0.9	Lab method on 0.0001-m^3 cores	0.9	0.1 (3.5 m), 0.5 (0.0 m), 0.9 (0.0 m)	0.1 (65%), 0.5 (100%), 0.9 (100%)
Mallants et al. (1997)	Udifluvent in orchard near Leuven, Belgium	variable with core volume	Lab method on 0.001-, 0.006- and 0.07-m^3 cores	1	0.001 m^3 (3.5 m), 0.006 m^3 (14), 0.07 m^3 (11 m)	0.001 m^3 (70%), 0.006 m^3 (45%), 0.07 m^3 (67%)
Mohanty and Mousli (2000)	Nicollet and Clarion loam in no-till agricultural area over glacial till	0.15, 0.3	Guelph permeameter and lab method on 0.0003-m^3 cores	4.6	0.15 (>90 m), 0.3 (60.5 m)	0.15 (52%), 0.3 (33%)
Sobieraj et al. (2002)	Brazilian rainforest catena with considerable textural diversity	0.2, 0.3, 0.5, 0.9	In situ with constant-head permeameter	25	0.9 (0 m), 0.3 (0 m), 0.5 (0 m), 0.9 (0 m)	0.9 (100%), 0.3 (100%), 0.5 (100%), 0.9 (100%)
Tsegaye and Hill (1998)	Aquic Hapludult for tilled area in Maryland	0.09, 0.3	Lab method on 0.00007-m^3 cores	1	0.09 (20 m), 0.30 (13 m)	0.09 (72%), 0.3 (69%)
Wilson and Luxmoore (1988), Wilson et al. (1989)	Walker Branch Watershed (WBW) Typic Paleudult, and Melton Branch Watershed (MBW) Typic Dystrochrept in forest setting	0, 0.95	In situ with tensiometer and Guelph permeameter	4, 4.2	WBW surface (0 m), WBW 0.95 (0 m); MBW surface (<15 m), MBW 0.95 (30 m)	WBW 0 (100%), WBW 0.95 (100%); MBW 0 (18%), MBW 0.95 (35%)

noisy spatial patterns of Ks primarily to the complex, small-scale biological processes within these forest soils.

This multi-scale study also has applications for hillslope and catchment modeling studies. As noted by Davis et al. (1999), Ks is one of the most sensitive input parameters in physically based hydrological models, and for their catchment study, they assigned a single value of Ks over large areas because Ks showed an apparently random distribution at lag intervals of 20 m. Davis et al. (1999, p. 687) state, however, that further work to assess the stochastic distribution of their experimental data set would provide additional information on the relative performance on how significant the spatial distribution of soil hydraulic properties is for the primary output of catchment discharge. Our multi-scale investigation assessing the stochastic distribution of the data set demonstrates that the assumption of a random distribution can be valid at some sampling scales but invalid at others.

Burrough (1983b) provides clear examples of nested semivariograms of soil physical properties that reflect the independent processes operating at different scales. Although there are multi-scale sources of spatial variation along this toposequnce, there were no nested semivariograms of Ks for transects 1 and 2, which capture the maximum variability along this toposequence. As already mentioned, we attribute this to the overriding effect of small-scale biological processes. An implication of our findings is that using soil texture as an indicator of spatial patterns of Ks across soilscapes can be invalid at some scales but valid at others, reinforcing the importance of multi-scale studies.

The experimental design used in this study is inefficient in terms of sampling effort. It is unlikely that many researchers have the resources to take thousands of Ks measurements. Pettitt and McBratney (1993) discuss differences in sampling efficiencies between model-based approaches using the variogram and geostatistical theory versus nested, design-based approaches where each randomly selected location has a fixed value. Although we adopted an inefficient model-based approach for this study, simple univariate statistics of random samples could have been effective in showing some of the spatial patterns of Ks between the sand-rich and clay-rich locations (e.g. Ks at 20 cm depth). Based on objectives and available resources, researchers may want to consider relatively efficient hybrid sampling designs (see Pettitt and McBratney, 1993), which can incorporate aspects of both model- and design-based approaches in capturing spatial variability at different sampling scales. This idea is worth further exploring.

6. Conclusions

This multi-scale study of a forested hillslope catena demonstrates that there is little autocorrelation in Ks at sampling scales ranging from lags of 25–0.25 m. A general lack of spatial structure in Ks suggests a predominance of small-scale processes, such as biological activity, that largely control water movement under saturated conditions. The spatial variability of Ks was similar to that of soil texture only when the sand component $\geq 80\%$, suggesting that textural macroporosity was more significant than bioporosity for extremely coarse textures. Common assumptions in modeling studies that assign Ks a random distribution in space may be valid at some scales but invalid at

others. Similarly, using soil texture as a first approximation of spatial patterns of Ks may be valid depending on the scale of observation. Because of its weak predictive capacity in forest soils, modelers must consider whether considerable time and effort in capturing small-scale spatial variability of Ks is necessary in accomplishing their objectives.

Acknowledgements

J. Sobieraj was in part supported by NSF grant no. 9554527 and by a grant from the Institute for Global Studies and Affairs at the University of Cincinnati. This study was only possible through logistical support and assistance by H. Schmitz.

References

Amoozegar, A., 1989a. A compact constant-head permeameter for measuring saturated hydraulic conductivity of the vadose zone. Soil Sci. Soc. Am. J. 53, 1356–1361.

Amoozegar, A., 1989b. Comparison of the Glover solution with the simultaneous-equations approach for measuring hydraulic conductivity. Soil Sci. Soc. Am. J. 53, 1362–1367.

Bosch, D.D., West, L.T., 1998. Hydraulic conductivity variability for two sandy soils. Soil Sci. Soc. Am. J. 62, 90–98.

Burrough, P.A., 1983a. Multiscale sources of spatial variation in soil: I. The application of fractal concepts to nested levels of soil variation. J. Soil Sci. 34, 577–597.

Burrough, P.A., 1983b. Multiscale sources of spatial variation in soil: II. A non-Brownian fractal model and its application in soil survey. J. Soil Sci. 34, 599–620.

Buttle, J.M., House, D.A., 1997. Spatial variability of saturated hydraulic conductivity in shallow macroporous soils in a forested basin. J. Hydrol. 203, 127–142.

Ciollaro, G., Romano, N., 1995. Spatial variability of the hydraulic properties of a volcanic soil. Geoderma 65, 263–282.

Clark, P.J., Evans, F.C., 1954. Distance to nearest neighbor as a measure of spatial relationships in populations. Ecology 35 (4), 445–453.

Cressie, N., Hawkins, D.M., 1980. Robust estimation of the variogram: I. Math. Geol. 12, 115–125.

Davis, S.H., Vertessy, R.A., Silberstein, R.P., 1999. The sensitivity of a catchment model to soil hydraulic properties obtained by using different measurement methods. Hydrol. Proc. 13 (5), 677–688.

Diggle, P.J., 1983. Statistical Analysis of Spatial Point Patterns. Academic Press, New York. 127 pp.

Eldridge, D.J., 1994. Nests of ants and termites influence infiltration in a semi-arid woodland. Pedobiologia 38, 481–492.

Goovaerts, P., 1997. Geostatistics for Natural Resource Evolution. Oxford Univ. Press, New York. 483 pp.

Iglewicz, B., 1983. Robust scale estimators and confidence intervals for location. In: Hoaglin, D.C., Mosteller, F., Tukey, J.W. (Eds.), Understanding Robust and Exploratory Data Analysis. Wiley, New York, pp. 404–429.

Isaaks, E.H., Srivastava, R.M., 1989. Applied Geostatistics. Oxford Univ. Press, Oxford. 561 pp.

Journel, A.G., Huijbregts, C.J., 1978. Mining Geostatistics. Academic Press, New York.

Kitanidis, P.K., 1997. Introduction to Geostatistics: Applications in Hydrogeology. Cambridge Univ. Press, New York.

Lauren, J.G., Wagenet, R.J., Bouma, J., Wosten, H.M., 1988. Variability of saturated hydraulic conductivity in a Glossaquic Hapludalf with macropores. Soil Sci. 145, 20–27.

Lee, K.E., 1985. Earthworms—Their Ecology and Relationships with Soils and Land Use. Academic Press, New York.

Litaor, I.M., Seastedt, T.R., Walker, D.A., 2002. Spatial analysis of selected soil attributes across an alpine topographic/snow gradient. Landsc. Ecol. 17, 71–85.

Lobry de Bruyn, L.A., Conacher, A.J., 1994. The effect of ant biopores on water infiltration in soils in undisturbed bushland and in farmland in a semi-arid environment. Pedobiologia 38, 193–207.

Mallants, D., Mohanty, B.P., Jacques, D., Feyen, J., 1996. Spatial variability of hydraulic properties in a multilayered soil profile. Soil Sci. 161 (3), 167–181.

Mallants, D., Mohanty, B.P., Vervoort, A., Feyen, J., 1997. Spatial analysis of saturated hydraulic conductivity in a soil with macropores. Soil Technol. 10 (2), 115–131.

McBratney, A.B., 1998. Some considerations on methods for spatially aggregating and disaggregating soil information. Nutr. Cycl. Agroecosyst. 50, 51–62.

McKeague, J.A., Wang, C., Topp, G.C., 1982. Estimating saturated hydraulic conductivity from soil morphology. Soil Sci. Soc. Am. J. 46, 1239–1244.

Mohanty, B.P., Mousli, Z., 2000. Saturated hydraulic conductivity and soil water retention properties across a soil-slope transition. Water Resour. Res. 36, 3311–3324.

Mohanty, B.P., Ankeny, M.D., Horton, R., Kanwar, R.S., 1994. Spatial analysis of hydraulic conductivity measured using disc infiltrometers. Water Resour. Res. 30, 2489–2498.

Oline, D.K., Grant, M.C., 2002. Scaling patterns of biomass and soil properties: an empirical analysis. Landsc. Ecol. 17, 13–26.

Pettitt, A.N., McBratney, A.B., 1993. Sampling designs for estimating spatial variance components. Appl. Stat. 42 (1), 185–209.

Ringrose-Voase, A.J., 1991. Micromorphology of soil structure: description, quantification, application. Aust. J. Soil Res. 29, 777–813.

Sobieraj, J.A., Elsenbeer, H., Marques, R., Newton, B., 2002. Spatial variability of soil hydraulic conductivity along a tropical rainforest catena. Geoderma 108 (1–2), 79–90.

Tsegaye, T., Hill, R.L., 1998. Intensive tillage effects on spatial variability of soil physical properties. Soil Sci. 163 (2), 143–154.

Wilson, G.V., Luxmoore, R.J., 1988. Infiltration, macroporosity, and mesoporosity distributions on two forested watersheds. Soil Sci. Soc. Am. J. 52, 329–335.

Wilson, G.V., Alfonsi, J.M., Jardine, P.M., 1989. Spatial variability of saturated hydraulic conductivity of the subsoil of two forested watersheds. Soil Sci. Soc. Am. J. 53, 679–685.